

Definition of Minimal Domains of Interaction Within the Recombination-Activating Genes 1 and 2 Recombinase Complex¹

Vassilis Aidinis,² Dora C. Dias, Carlos A. Gomez, Debika Bhattacharyya, Eugenia Spanopoulou,³ and Sandro Santagata⁴

During V(D)J recombination, recognition and cleavage of the recombination signal sequences (RSSs) requires the coordinated action of the recombination-activating genes 1 and 2 (RAG1/RAG2) recombinase complex. In this report, we use deletion mapping and site-directed mutagenesis to determine the minimal domains critical for interaction between RAG1 and RAG2. We define the active core of RAG2 required for RSS cleavage as aa 1–371 and demonstrate that the C-terminal 57 aa of this core provide a dominant surface for RAG1 interaction. This region corresponds to the last of six predicted kelch repeat motifs that have been proposed by sequence analysis to fold RAG2 into a six-bladed β -propeller structure. Residue W317 within this sixth repeat is shown to be critical for mediating contact with RAG1 and concurrently for stabilizing binding and directing cleavage of the RSS. We also show that zinc finger B (aa 727–750) of RAG1 provides a dominant interaction domain for recruiting RAG2. In all, the data support a model of RAG2 as a multimodular protein that utilizes one of its six faces for establishing productive contacts with RAG1. *The Journal of Immunology*, 2000, 164: 5826–5832.

The ability of the adaptive immune system to recognize and respond to innumerable foreign Ags is dependent upon clonotypic Ag receptors expressed on the surface of T and B lymphocytes. The vast Ag receptor repertoire is generated by the somatic assembly of composite gene segments in a process termed V(D)J recombination (reviewed in Refs. 1 and 2). Rearrangement of these gene segments is directed by highly conserved recombination signal sequences (RSSs)⁵ consisting of a heptamer (CA-CAGTG) and a nonamer (ACAAAAACC) motif separated by a 12- or 23-bp spacer. Efficient recombination occurs between two gene segments flanked by RSSs with different spacer lengths (3).

Recombination is initiated by two lymphoid-specific factors, recombination-activating genes 1 and 2 (RAG1 and RAG2) (4, 5). These genes are located 8 kb apart within the same genomic locus and were first identified by their capacity to activate rearrangement of an artificial substrate in a fibroblast cell line. Functional disruption of either gene by either homologous recombination in mice (6, 7) or by amino acid substitutions or truncations in humans

with severe combined immunodeficiency or Omenn syndrome (8–10) has confirmed the fundamental role of RAGs in V(D)J recombination.

Numerous aspects of the recombination reaction are dependent upon the interplay between RAG1 and RAG2 during the rearrangement process. Although RAG1 has recently been shown to contain the catalytic residues of the recombinase and can alone bind the RSS in part through a helix-turn-helix motif homologous to the DNA binding domain of the Hin recombinase (11–15), such a complex cannot mediate DNA nicking (16–18). Upon recruitment of RAG2, contacts between the recombinase and the RSS are modified (13, 14, 19, 20), resulting in stabilization of the recombinase-RSS complex (21, 22) and bending of the RSS (23), with significant distortion of the heptamer coding flank border (19, 20). The interaction of RAG2 with RAG1 likely triggers a conformational change in RAG1 that activates its hydrolytic machinery and targets nicking at the border of the RSS and the coding flank. The free hydroxyl group of the nicked strand is then used in a transesterification reaction by the RAG1/RAG2 complex to form a covalently sealed hairpin (24). The hydrolytic mechanism of the RAG1/RAG2 recombinase is again employed for resolving the hairpin intermediate (25, 26) and for processing numerous 3' overhang structures (27). The minimal regions of both proteins that are sufficient for mediating recombination *in vivo* are referred to as the active cores and span residues 384–1008 in RAG1 (28) and residues 1–383 in RAG2 (24, 29).

Substantial evidence suggests that most steps of V(D)J recombination occur with the 12 and 23 RSSs juxtaposed in a tightly regulated synaptic complex (30–35). Formation and maintenance of this complex in which double strand breaks are generated requires both RAG1 and RAG2. Following cleavage, both RAGs are integral components of the postcleavage complex (33, 36). In addition, in a reaction paralleling the mechanism used by transposases, the postcleavage complex of RAG1 and RAG2 can transpose cut signal ends into unrelated DNA via a nucleophilic attack (37, 38).

Ruttenberg Cancer Center, Mount Sinai School of Medicine, New York, NY 10029
Received for publication November 5, 1999. Accepted for publication March 22, 2000.

The costs of publication of this article were defrayed in part by the payment of page charges. This article must therefore be hereby marked *advertisement* in accordance with 18 U.S.C. Section 1734 solely to indicate this fact.

¹ This work was supported by National Institutes of Health Grant AI40191 and Cancer Research Institute Investigator Award (to Zhen-Qiang Pan). S.S. was supported by a predoctoral training grant in Cancer Research from the National Institutes of Health. D.C.D. was supported by Praxis XXI/BD/13442/97 fellowship awarded by the Foundation for Science and Technology (Portugal).

² Current address: Hellenic Pasteur Institute, Laboratory of Molecular Genetics, 127 Vas. Sofias Avenue, 11521 Athens, Greece

³ Eugenia Spanopoulou died on September 2, 1998.

⁴ Address correspondence and reprint requests to Dr. Sandro Santagata, Mount Sinai School of Medicine, Ruttenberg Cancer Center, Box 1130, 1425 Madison Avenue, New York, NY 10029. E-mail address: santas01@doc.mssm.edu

⁵ Abbreviations used in this paper: RSS, recombination signal sequence; RAG, recombination-activating gene; ZFB, zinc finger B; ZFA, zinc finger A.

The multifaceted capacities of the RAG1/RAG2 complex for directing DNA recognition before alternating hydrolysis, transesterification, and hydrolysis reactions within a regulated synaptic complex suggest a dynamic interface between RAG1 and RAG2. This interaction has previously been explored in a number of ways. The RAG proteins have been observed to colocalize in the periphery of the nucleus of thymocytes by indirect immunofluorescence and have been coprecipitated from thymocytes as well as from various cell lines transiently overexpressing the RAG proteins (39, 40). In addition, reconstitution experiments using purified RAG1 and RAG2 have demonstrated a direct interaction between the two proteins in the absence of DNA (22, 41). Mapping of the domains of interaction between RAG1 and RAG2 has been undertaken only in part, with aa 504–1008 of RAG1 shown to complex with RAG2 (aa 1–491) (40). RAG2, which has recently been suggested by sequence analysis to form a β -propeller-like structure composed of six kelch repeat motifs (42, 43), has not been further subjected to deletional mapping.

In this study, we report a detailed analysis of the dominant domains of interaction between the active cores of RAG1 and RAG2. We show that the predicted sixth kelch motif of RAG2 is largely responsible for mediating interaction with RAG1 and that mutation of amino acid W317 within this region abolishes complex formation between RAG1 and RAG2 with subsequent deleterious effects on RSS recognition and cleavage. Moreover, we show that zinc finger B (ZFB) at the C terminus of RAG1 is involved in recruitment of RAG2. In all, these data complement and extend our view of the importance of RAG1-RAG2 interactions for the activation of V(D)J recombination and provide a view of RAG2 as a modular adapter protein.

Materials and Methods

Recombinant plasmid constructs and mutagenesis

GST fusion constructs were generated by subcloning *Bam*HI/*Not*I-digested PCR products of RAG1 and RAG2 into the eukaryotic expression vector pEBG, which is under the transcriptional regulation of the elongation factor 2 promoter (39). Amino acid substitutions within RAG2 were generated in pBluescript using the Bio-Rad (Richmond, CA) Phagemid kit and were transferred as *Kpn*I/*Ear*I fragments into pEBG2AC (11). All constructs were sequenced.

RAG1 and RAG2 interaction assays

Recombinant proteins were overexpressed in the human embryonic kidney fibroblast cell line HEK293T by calcium phosphate transfection (39). Cells were harvested 48 h posttransfection in PBS and subsequently lysed in IP lysis buffer (25 mM Tris-HCl (pH 8.0); 250 mM NaCl; 1 mM MgCl₂; 0.5% Nonidet P-40; 5% glycerol; and 2 μ g/ml of the aprotinin, leupeptin, and pepstatin protease inhibitors). Extracts were spun down for 10 min at 4°C, and the supernatants were incubated with 20 μ l of pre-equilibrated GST beads for 2 h at 4°C with rocking. Beads were washed five times in IP-lysis buffer, resuspended in SDS gel-loading buffer (50 mM Tris-HCl (pH 6.8), 100 mM DTT, 2% SDS, 0.1% bromophenol blue, and 10% glycerol), and boiled for 10 min at 95°C. Proteins were then resolved by SDS/PAGE and transferred to nitrocellulose membranes that were blocked by a 30-min incubation in TBST-1% milk. Membranes were incubated with the primary mAb (anti-HA (1:200 dilution) and/or anti-GST (1:1000 dilution)) for 2 h in TBST-1% milk before three washes. Membranes were then incubated with secondary Ab (conjugated with either alkaline phosphatase or HRP) for 30 min. Protein bands were visualized by incubation either with the alkaline phosphatase substrate (Promega, Madison, WI) or with luminol (enhanced chemiluminescence system; Amersham, Arlington Heights, IL).

Protein expression and purification

GST fusions of RAG1 and RAG2 were overexpressed in HEK293T cells and purified as previously described (11). Proteins were dialyzed in cleavage buffer (25 mM Tris-HCl (pH 8.0), 150 mM KCl, 2 mM DTT, and 20% glycerol), quantified by Coomassie blue staining after SDS/PAGE, and stored at –80°C in single-use aliquots.

Oligonucleotide DNA cleavage substrates

The 12-RSS upper-strand oligonucleotide (22) was 5' end-labeled with γ -³²P ATP using T4 polynucleotide kinase (NEB, Beverly, MA) as described by the manufacturer. The unlabeled lower-strand was then annealed by incubation at 75°C for 2 min before slow cooling to room temperature. The unincorporated nucleotides were removed by passage through a Sepharose spin column (G-50 or G-25; Boehringer Mannheim, Indianapolis, IN), and the double-stranded, radiolabeled substrates were then ethanol precipitated and resuspended at a concentration of 0.05 pmol/ μ l.

In vitro cleavage reactions

Cleavage reactions were performed essentially as described (22, 24). A total of 100 ng of RAG1 and RAG2 were incubated for 90 min at 37°C with 0.05 pmols of ³²P-labeled 12 RSS in 12.5 mM MOPS-KOH (pH 7.0), 5 mM Tris-HCl (pH 7.0), 30 mM KCl, 60 mM KOAc, 1.4 mM DTT, 0.5 μ M nonspecific single-stranded DNA, 0.05 μ g/ μ l BSA, 10% DMSO, 4% glycerol, and 0.5 mM MgCl₂ or MnCl₂ in a final volume of 20 μ l. Reactions were stopped by the addition of 0.1% SDS and denaturing gel-loading buffer (98% deionized formamide, 10 mM EDTA (pH 8.0), 0.025% xylene cyanol FF, and 0.025% bromophenol blue) and were resolved on 16% polyacrylamide/6 M urea denaturing gels.

EMSA

Conditions were essentially as previously described (21, 22). A total of 50 ng of RAG1 and RAG2 were incubated with 0.05 pmols of ³²P-labeled 12 RSS at 30°C for 10 min in 25 mM MOPS-KOH (pH 7.0), 5 mM Tris-HCl (pH 7.0), 30 mM KCl, 120 mM KOAc, 2.4 mM DTT, 1 μ M nonspecific single-stranded DNA, 0.1 μ g/ μ l BSA, 20% DMSO, 4% glycerol, and 1 mM MgCl₂ in a final volume of 10 μ l. The complexes were then cross-linked by addition of 1 μ l glutaraldehyde (final concentration, 0.1% v/v) and incubated for 10 min at 30°C. Complexes were resolved on 4% native polyacrylamide gels.

In vivo recombination assays

In vivo recombination assays were performed in HEK293T cells essentially as previously described (9, 23). HEK293T (or HEK293, NIH3T3) cells were cotransfected with the deletional recombination substrate pJH289 (5 μ g) (44) and 6 μ g of the expression vectors for GST-RAG1 Δ N330 and the various GST-RAG2 mutants. Cells were harvested 48 h posttransfection, and DNA was isolated as described (5) and analyzed for recombination frequency by PCR analysis (20 cycles of 94°C for 30 s, 65°C for 60 s, and 74°C for 60 s). The linear range of the PCR assay was determined by serial dilutions of the rescued recombined plasmid. A total of 0.2% of the recovered plasmid was used in all assays. Oligonucleotides detect the recombined products by annealing to the joined signal ends and to the CAT gene present in pJH289 (oligos RA5 and RA14, respectively) (45, 46). As a loading control, a 154-bp fragment of the CAT gene was amplified (oligos RA1 and RA14) (23) under identical conditions (data not shown). Amplified products were visualized by autoradiography after electrophoresis on a 10% polyacrylamide gel.

Results and Discussion

Definition of the minimum RAG2 domain for RAG1 coprecipitation

To identify the region of RAG2 required for coprecipitation of RAG1, a panel of RAG2 deletion mutants was constructed as GST N-terminal fusions (Fig. 1A). The GST tag not only facilitates detection and purification of the recombinant proteins but also provides increased solubility and/or stability while leaving recombination activity of episomal substrates essentially unaltered (39). The recombinant forms of GST-RAG2 were transiently overexpressed in the human kidney fibroblast cell line HEK293T, together with an N-terminal HA-tagged form of the RAG1 active core (HA-RAG1 Δ N330–1040). GST-RAG2 proteins were purified from the cell extracts on glutathione-agarose beads, and coprecipitation of RAG1 was evaluated by Western blot analysis. Equivalent levels of RAG1 expression in each assay were confirmed by blotting total cellular extracts (data not shown). Both the full-length (aa 1–527) and active core (aa 1–388) forms of RAG2 were able to efficiently coprecipitate RAG1 (Fig. 1B, lanes 1 and 2), whereas GST alone did not associate with RAG1 (lane 7).

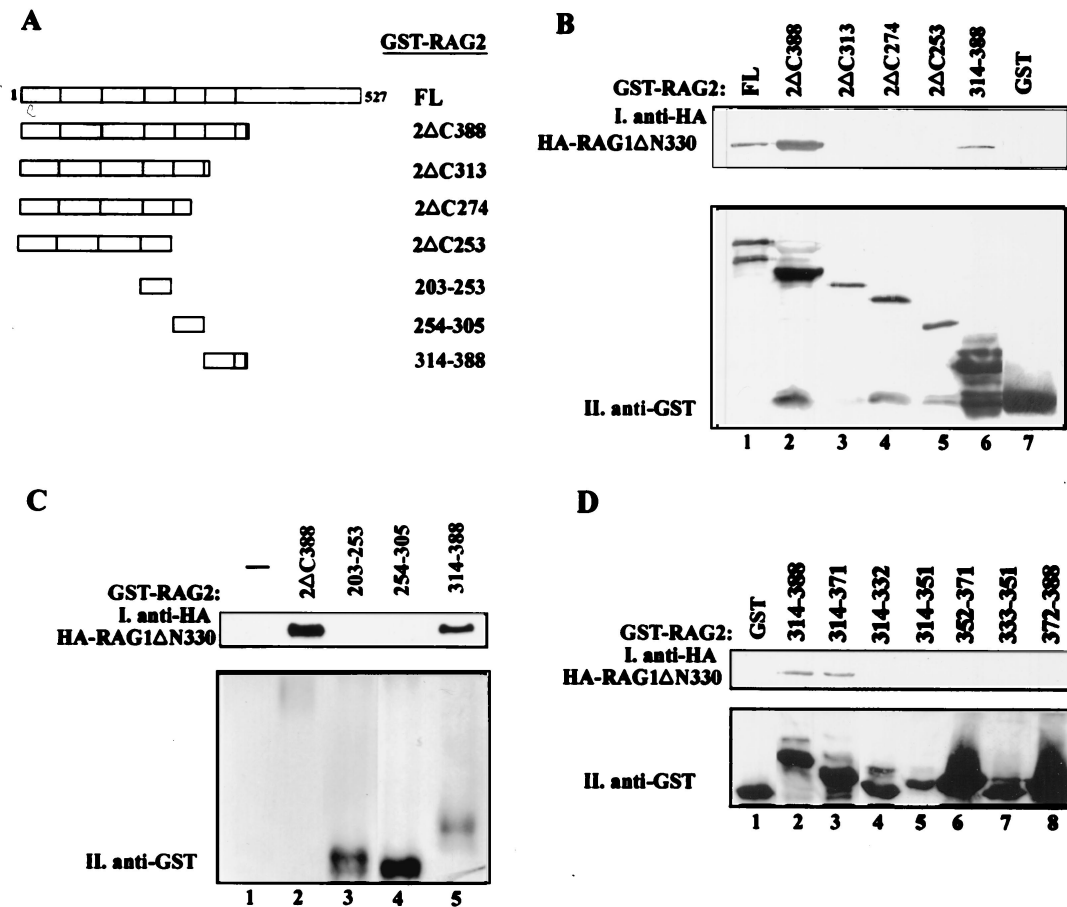


FIGURE 1. The predicted sixth kelch repeat motif of RAG2 coprecipitates RAG1. **A**, Schematic representation of the RAG2 deletion mutants used to define the minimal domain of interaction required for RAG1 coprecipitation. Vertical lines at amino acid positions 61, 128, 201, 253, 305, and 351 define the six fold repeats of the kelch motifs. **B**, Amino acids 314–388 of RAG2 are sufficient for coprecipitation of RAG1. 293T cells were cotransfected with HA-tagged RAG1ΔN330 and various GST-tagged RAG2 deletion mutants described in **A**. Cell extracts were incubated with glutathione beads, and the purified proteins were transferred to a nitrocellulose filter after SDS/PAGE. The filter was sequentially incubated, as described in *Materials and Methods*, with an anti-HA Ab and then with an alkaline phosphatase-conjugated secondary Ab and an anti-GST Ab before a HRP-conjugated secondary Ab. **C**, Putative repeats 4 and 5 of RAG2 are unable to effectively coprecipitate RAG1. GST-tagged forms of the RAG2 active core (aa 1–388) as well as repeats 4, 5, and 6 were assayed for the capacity to interact with HA-tagged RAG1ΔN330. The borders of the individual repeats were generated according to the structural predictions of Callebaut and Moron (42) and Aravind and Koonin (43). Repeat 4, aa 203–253; repeat 5, aa 254–305; repeat 6, aa 314–388. The GST-tagged RAG2 forms were coexpressed with HA-tagged RAG1ΔN330 in 293T cells, purified on glutathione beads, and analyzed by Western blotting as in **B**. **D**, Amino acids 314–371 span the minimal domain of RAG2 required for RAG1 coprecipitation. GST-tagged RAG2 peptides were coexpressed with HA-tagged RAG1ΔN330, purified on glutathione beads, and evaluated by Western blot analysis as described in **B**. FL, Full-length aa 1–527.

Deletion of aa 314–388 entirely abolished precipitation of RAG1 (lane 3) and, accordingly, further deletions of the RAG2 core were also unable to associate with RAG1 (lanes 4 and 5). These findings suggest that aa 314–388 are involved in mediating interaction with RAG1, and indeed a peptide spanning this region successfully precipitated RAG1, albeit at somewhat reduced levels (lane 6). To exclude the possibility that the RAG1-RAG2 association was mediated through nonspecific binding of contaminating genomic DNA, the above interactions were analyzed in the presence of ethidium bromide, which disrupts protein interactions mediated through DNA (47). In fact, RAG1/RAG2/RSS complexes can be entirely disrupted with 100 $\mu\text{g/ml}$ ethidium bromide as determined by mobility shift analysis (data not shown). Because the presence of 400 $\mu\text{g/ml}$ ethidium bromide did not alter the level of association between aa 314–388 of RAG2 and RAG1 (data not shown), we conclude that the interaction of RAG2 with RAG1 is not mediated through nonspecific DNA binding.

To further assess whether other predicted kelch repeats were capable of associating with RAG1, we generated fusions of the

fourth and fifth repeats to GST and repeated the coprecipitation experiments described above. Although the active core (aa 1–388) of RAG2 and the sixth repeat were able to coprecipitate, the RAG1 active core (HA-RAG1ΔN330–1040) (Fig. 1C, lanes 2 and 5) repeats 4 (205–253) and 5 (254–305) were unable to efficiently precipitate RAG1 (Fig. 1C, lanes 3 and 4). The current data suggest that the predicted sixth kelch repeat of RAG2 provides a dominant interface of interaction with RAG1. However, the effectiveness of such an experiment is dependent upon the selection of appropriate borders for each of the repeats. Hence, we cannot entirely exclude the possibility that RAG2 may in part use one of the other repeats for making contacts with RAG1.

To further define the minimum RAG2 domain required for coprecipitation of RAG1, a series of GST fusion peptides spanning the interaction site was constructed. Only the peptides encompassing aa 314–388 and 314–371 (Fig. 1D, lanes 2 and 3) were able to coprecipitate RAG1, indicating that the minimum domain of interaction is between aa 314 and 371. Recently, sequence analysis has revealed that RAG2 possesses a six-fold symmetrical structure

Table I. A summary of the properties of RAG2 mutant proteins^a

GST-RAG2	RAG1 Co-P	In vitro Cleavage	In vivo Recombination
Full length	+	+	+
2ΔC388	+	+	+
2ΔC371	+	+	+
2ΔC313	-	-	-
314-388	+	-	-
2ΔC388 W317Y	-	-	-
2ΔC388 F318Y	+	+	+
2ΔC388 WF317/8YY	-	-	-

^a RAG1 coprecipitation assays (Co-P) as described in Figs. 1, 3, and 4. In vitro cleavage assays are as described in Fig. 2B. In vivo recombination assays: the expression vectors of the indicated proteins were cotransfected with the exogenous recombination substrate pJH289 in 293T cells. A fragment of the recombined plasmids was detected by a semiquantitative PCR assay, as described in *Materials and Methods* and Ref. 23.

with each repeat composed of a kelch motif (42, 43). Intriguingly, aa 314-371 coincide with the sixth kelch motif. Crystallographic analysis has revealed that the ~50-aa kelch motif acquires a fold consisting of four β strands, which is reminiscent of the superbarrel fold observed in the proteins of the sialidase family (48, 49). Kelch motifs have been observed in numerous proteins, including galactose oxidase from *Dactylium dendroides* (48), the α - and β -scruin proteins from *Limulus polyhemus* (50), the kelp protein involved in cell fusion and morphology in *Saccharomyces cerevisiae* (51), the kelch protein of *Drosophila* that is involved in cytoplasmic transport from nurse cells to oocytes (52), and the mouse *IAP-promoted placental (MIPP) protein* (53). Our finding that a single kelch motif can mediate protein-protein interactions between RAG2 and RAG1 support the model that RAG2 is indeed composed of six discrete repeats formed from four antiparallel β strands. Predominant contact with RAG1 through the C-terminal kelch motif suggests that the N-terminal five repeats may be available to establish interactions with other proteins involved in the V(D)J recombination reaction. Because kelch associates with actin in the ring canals in *Drosophila* egg chambers (54) and α - and β -scruin are actin-bundling proteins (55), it is exciting to speculate that RAG2 may localize the recombinase to the nuclear periphery by binding structural components of the nuclear matrix through one of its kelch motifs. A capacity to form discrete contacts through individual blades of a putative β -propeller would imply that RAG2 may function as a multimodular adapter protein involved in coordinating macromolecular assemblies during the recombination process.

In previous studies, mutational and deletional analyses have demonstrated that aa 1-383 of RAG2 are essential for RAG1/RAG2-mediated recombination of episomal substrates in transiently transfected cells (29, 56). Because aa 372-388 are dispensable for interaction between RAG2 and RAG1, we next examined whether they are also nonessential for RAG1/RAG2-mediated RSS binding and cleavage. A GST fusion of the RAG2 active core spanning aa 1-371 (RAG2ΔC371), as expected, was able to efficiently precipitate RAG1 (Table I). Accordingly, along with RAG1, RAG2ΔC371 displayed comparable activity to RAG2ΔC388 for complex formation on the 12 RSS (Fig. 2A, lanes 3 and 7), for 12 RSS cleavage (Fig. 2B, lanes 3, 7, 13, and 17), and for in vivo recombination of an exogenous substrate (Table I). Thus, we conclude that the minimal active core of RAG2 required for both in vitro and in vivo activity spans aa 1-371. Deletion of the region corresponding to the predicted sixth kelch motif (RAG2ΔC313), which abolishes formation of the RAG1/RAG2 complex, abolished entirely both 12 RSS binding (Fig. 2A, lane 8)

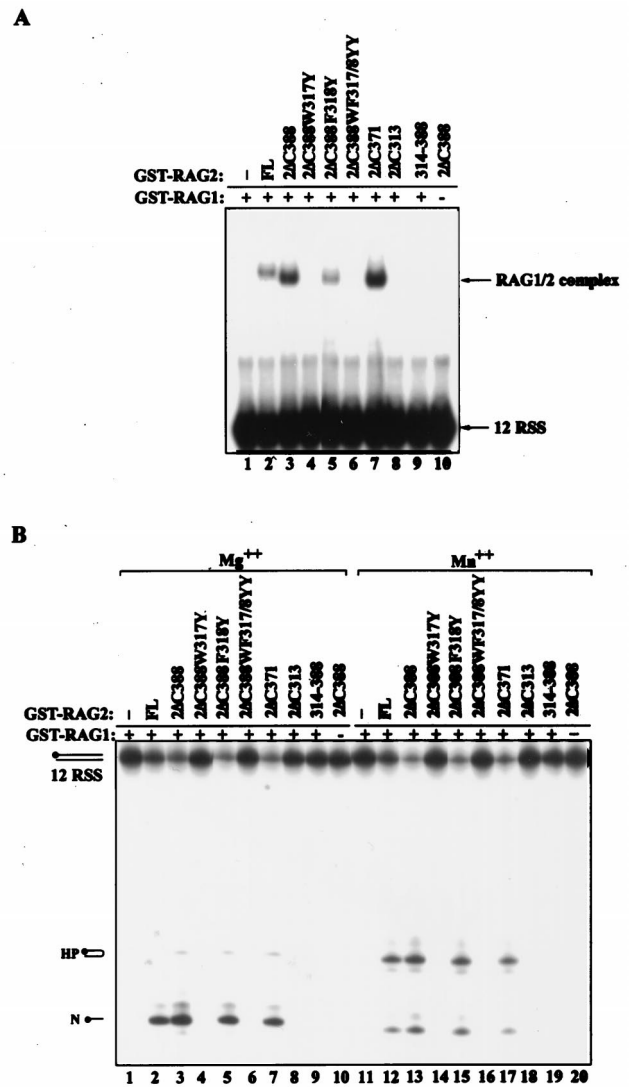
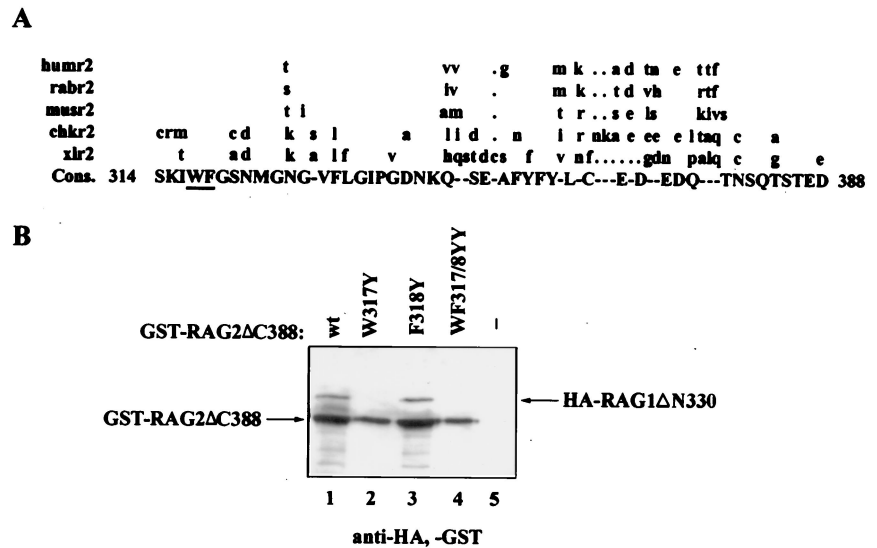


FIGURE 2. Interaction of RAG2 and RAG1 is essential for RSS binding and cleavage. *A*, Interaction of RAG2 with RAG1 is required for efficient RSS binding. EMSAs: 50 ng of purified GST-RAG1ΔN380 (active core) and 50 ng of purified deletional or mutational forms of GST-RAG2 were incubated with 0.05 pmols of a 12-RSS oligonucleotide substrate 5' end-labeled on the upper strand. Complexes were analyzed on a 4% native polyacrylamide gel and visualized by autoradiography. *B*, Interaction of RAG2 and RAG1 is essential for RSS cleavage. In vitro cleavage assays were performed using 0.05 pmols of a 12 RSS end-labeled on the 5' end of the upper strand in 0.5 mM of either Mg²⁺ or Mn²⁺. The substrates were incubated with 100 ng of purified GST-RAG1ΔN380, and equimolar amounts of purified deletional or mutational forms of GST-RAG2 as described in the *Materials and Methods*. Products (N, nick; HP, hairpin) were analyzed on a 16% polyacrylamide/6 M urea denaturing gel.

and cleavage activity (Fig. 2B, lanes 8 and 18), thus demonstrating the importance of this region for establishing a productive DNA binding and cleavage complex. However, although the putative sixth kelch domain alone could coprecipitate RAG1, it could not activate the DNA recognition (Fig. 2A, lane 9) and hydrolytic mechanisms (Fig. 2B, lanes 9 and 19) of the recombinase, indicating that the first five kelch motifs are also critical for the activity of the RAG1/RAG2 complex. In all, the data demonstrate that although the sixth kelch repeat is capable of interacting with RAG1, it is not sufficient for activating the catalytic capacity of RAG1 to initiate the first steps of the recombination reaction.

FIGURE 3. W317 of the putative sixth RAG2 kelch motif is critical for RAG1 binding. **A**, The amino acid sequences of the sixth kelch motifs of RAG2 from five species (human, rabbit, mouse, chicken, and xenopus) are aligned above the consensus sequence (adopted from Sadofsky et al. (56)). **B**, Coprecipitation of RAG1 is eliminated by mutation W317Y. GST-tagged RAG2 Δ C388 carrying wild-type (wt) or mutated sequences was coexpressed with HA-tagged RAG1 Δ N330 in 293T cells, purified on glutathione beads, and analyzed by Western blot as described in Fig. 1. The nitrocellulose filter was simultaneously blotted with anti-HA and anti-GST Abs.



Tryptophan 317 of RAG2 is critical for establishing contact with RAG1

To identify amino acid residues within the proposed sixth kelch motif of RAG2 that are potentially critical for mediating interaction with RAG1, we compared the sequences of all known RAG2 molecules from various species. Interestingly, limited sequence conservation is observed in this region (Fig. 3A). W317 and F318 are among the most conserved residues. We explored the role of these two residues in RAG1/RAG2 complex formation by introducing the conservative amino acid substitutions WF317/8YY. After coexpression in 293T cells, RAG2 Δ C(WF317/8YY) was unable to coprecipitate RAG1 (Fig. 3B, lane 4). Single amino acid mutations RAG2 Δ CW317Y and RAG2 Δ CF318Y revealed that W317 is essential for coprecipitation of RAG1, whereas mutation F318Y did not interfere with RAG1 interaction (Fig. 3B, lanes 2 and 3). Functional analysis of W317Y demonstrated that disruption of RAG1 interaction concurrently abolished 12 RSS binding (Fig. 2A, lane 4) and cleavage (Fig. 2B, lanes 4 and 14) as well as the capacity for in vivo recombination (Table I). On the other hand, F318Y, which was capable of interacting with RAG1, also permitted complex formation on the 12 RSS (Fig. 2B, lane 5), efficient 12 RSS cleavage (Fig. 2B, lanes 5 and 15), and in vivo recombination (Table I).

Complete disruption of RAG1/RAG2 complex formation by the W317Y substitution prompts at least two potential explanations. One possibility is that the tryptophan might directly participate at the interaction interface to stabilize contacts between RAG1 and RAG2. Interestingly, such a role for tryptophans has been observed in the crystal structures of the bacteriophage Mu transposase, where W279 and F280 mediate subdomain interactions (57), and of N-cadherins, where the dimer interface is coordinated by intercalation of the W2 side chain into the hydrophobic pocket of a partner molecule. (58). Alternatively, because tryptophans can serve as integral structural components within the architecture of a protein, W317Y might unstructure RAG2. This possibility appears unlikely because W317Y did not modify the nuclear localization pattern of RAG2 (data not shown).

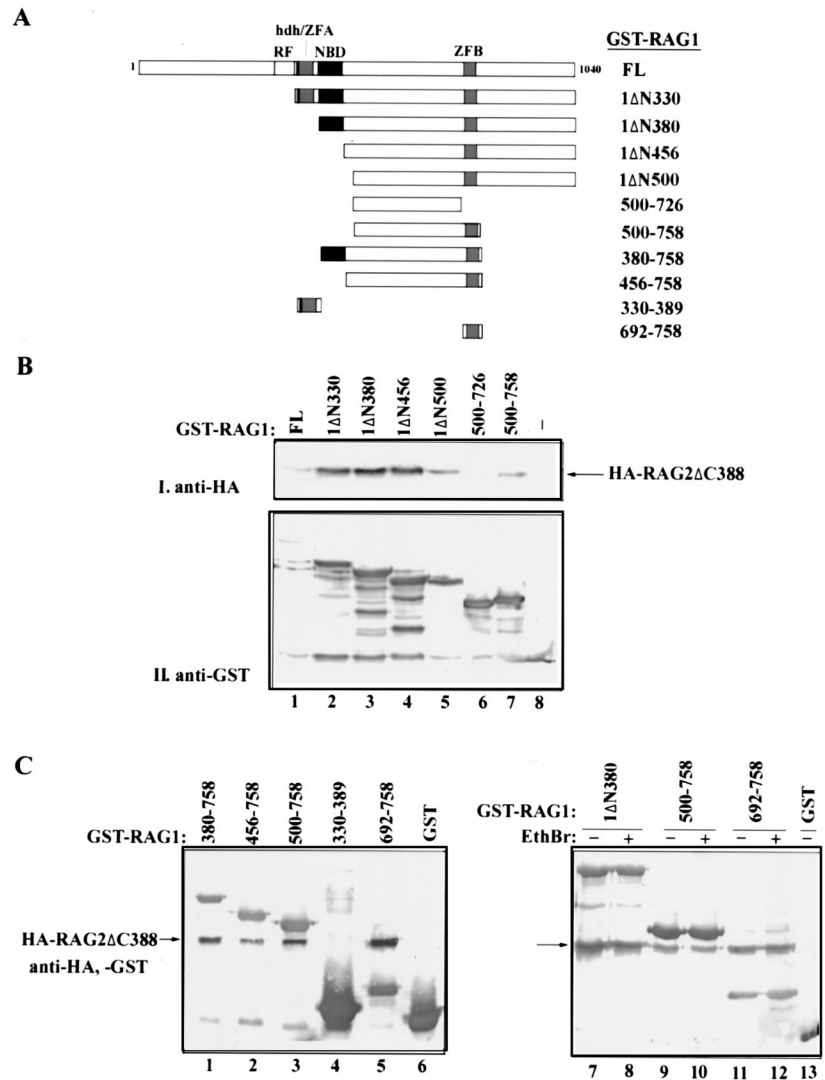
RAG1 ZFB is involved in RAG1-RAG2 DNA-independent interaction

Having established a predominant RAG2 domain involved in the interaction with RAG1, we sought to further define the regions of

RAG1 required for coprecipitation of RAG2. McMahan et al. (40) have previously identified a large region of RAG1 spanning aa 504–1008 that is able to precipitate RAG2 after overexpression in COS cells. This region has been shown to contain a single C₂H₂ zinc binding domain (ZFB, aa 727–750), which possesses weak and apparently nonspecific DNA binding capacity (59). The N terminus of RAG1, which is dispensable for in vivo recombination, contains two zinc binding domains (a ring finger and a zinc finger A (ZFA)), which together form a highly specific dimerization interface between RAG1 molecules (59, 60). Due to the ability of the N-terminal zinc binding domains to coordinate protein interactions, we tested the role of ZFB in mediating RAG1 and RAG2 interaction.

A series of GST-fused RAG1 deletion mutants was generated (Fig. 4A) and coexpressed with an HA-tagged form of the RAG2 active core (HARAG2 Δ C388) in HEK293T cells. Complexes were purified on glutathione beads, and coprecipitation of RAG2 was detected by Western blot analysis. In agreement with McMahan et al. (40), the C terminus of RAG1 (aa 500–1040) was able to coprecipitate RAG2 (Fig. 4B, lane 5). Deletion of aa 758–1040 (aa 500–758), which left ZFB intact, had no effect on the interaction with RAG2 (Fig. 4B, lane 7, and C, lane 3), whereas a further deletion of aa 726–1040, which completely removes ZFB, abolished the interaction (Fig. 4B, lane 6). Moreover, a peptide encompassing ZFB (aa 692–758) was still able to coprecipitate RAG2 (Fig. 4C, lane 5), whereas a peptide spanning the N-terminal C₂H₂ zinc-binding motif ZFA (aa 330–389) and GST alone failed to interact with RAG2 (Fig. 4C, lanes 4 and 6). Because the interaction between ZFB and RAG2 was unaltered by the introduction of 400 μ g/ml ethidium bromide (Fig. 4C, lane 12), we conclude that the recruitment of RAG2 by ZFB of RAG1 is not mediated through nonspecific DNA binding. Equal levels of RAG2 expression in all of the assays presented in Fig. 4 were evaluated by blotting crude extracts (data not shown). Although ZFB represents a predominant interface of interaction, our data do not permit us to exclude the possibility that RAG1 and RAG2 interactions are established through other domains present in RAG1. In addition, attempts to determine whether the sixth kelch motif of RAG2 directly interacts with ZFB of RAG1 were hampered by the poor solubility of both short peptides when expressed as HA-tagged forms (data not shown).

FIGURE 4. RAG1 ZFB coprecipitates the RAG2 active core. *A*, Schematic representation of the RAG1 deletion mutants used in *B* and *C*. *B*, Amino acids 500–758 of RAG1 are capable of precipitating the RAG2 active core. The 293T cells were cotransfected with HA-tagged RAG2 Δ C388 and the various GST-tagged RAG1 deletion mutants described in *A*. Cell extracts were incubated with glutathione beads, and the purified proteins were transferred to a nitrocellulose filter after SDS/PAGE. The filter was sequentially incubated, as described in the *Materials and Methods*, with 1) an anti-HA Ab and then an alkaline phosphatase-conjugated secondary Ab and 2) an anti-GST Ab and then a HRP-conjugated secondary Ab. *C*, ZFB of RAG1 is sufficient to precipitate RAG2. The interaction was evaluated as described in *B*. The nitrocellulose filters were simultaneously blotted with anti-HA and anti-GST Abs. The interaction assays presented in *lanes 7–13* were performed in the presence (+) or absence (–) of 400 μ g/ml ethidium bromide (EthBr). FL, Full-length; RF, ring finger aa 288–330; hdh, homodimerization helices aa 340–351; ZFA, ZFA aa 353–374; NBD, nonamer binding domain aa 389–446; ZFB, ZFB aa 727–750.



The capacity of RAG2 to interact with the nonspecific DNA binding component ZFB suggests a model in which RAG2 promotes spacer and heptamer occupancy by binding to and reorienting ZFB (13, 14, 20). In the absence of RAG2, ZFB and the catalytically critical residues of RAG1 might be configured on the RSS in an inactive conformation. Complex formation between RAG2 and ZFB could redirect ZFB out toward the heptamer where the zinc finger would then stabilize the RAG1/RAG2 ternary complex through extensive interactions with both RAG2 and with conserved and nonconserved motifs within the RSS, thereby permitting an optimal state for DNA nicking and transesterification.

In this study we present minimal domains in RAG1 and RAG2 required for efficient complex formation. Whether these domains are central for all the steps of RSS recognition, synapsis, and cleavage or whether different interfaces of interaction are utilized for each step of the reaction remains to be addressed. Nonetheless, the deletion mapping of the interaction domains between RAG1 and RAG2 presented in this study provides an important first step toward an understanding of the intricate contacts required to form a RAG1/RAG2 complex that is active for RSS binding and cleavage.

Acknowledgments

We thank Stuart Aaronson, Patricia Cortes, and Zhen-Qiang Pan for their kind support, Chris Roman for providing single-stranded RAG2 cDNA, and Benedicte Py for help with subcloning.

References

- Grawunder, U., R. B. West, and M. R. Lieber. 1998. Antigen receptor gene rearrangement. *Curr. Opin. Immunol.* 10:172.
- Lewis, S. M. 1994. The mechanism of V(D)J joining: lessons from molecular, immunological, and comparative analyses. *Adv. Immunol.* 56:27.
- Tonegawa, S. 1983. Somatic generation of antibody diversity. *Nature* 302:575.
- Schatz, D. G., M. A. Oettinger, and D. Baltimore. 1989. The V(D)J recombination activating gene, RAG-1. *Cell* 59:1035.
- Oettinger, M. A., D. G. Schatz, C. Gorka, and D. Baltimore. 1990. RAG-1 and RAG-2, adjacent genes that synergistically activate V(D)J recombination. *Science* 248:1517.
- Mombaerts, P., J. Iacomini, R. S. Johnson, K. Herrup, S. Tonegawa, and V. E. Papaioannou. 1992. RAG-1-deficient mice have no mature B and T lymphocytes. *Cell* 68:869.
- Shinkai, Y., G. Rathbun, K. P. Lam, E. M. Oltz, V. Stewart, M. Mendelsohn, J. Charron, M. Datta, F. Young, A. M. Stall, et al. 1992. RAG-2-deficient mice lack mature lymphocytes owing to inability to initiate V(D)J rearrangement. *Cell* 68:855.
- Schwarz, K., G. H. Gauss, L. Ludwig, U. Pannicke, Z. Li, D. Lindner, W. Friedrich, R. A. Seger, T. E. Hansen-Hagge, S. Desiderio, M. R. Lieber, and

- C. R. Bartram. 1996. RAG mutations in human B cell-negative SCID. *Science* 274:97.
9. Villa, A., S. Santagata, F. Bozzi, S. Giliani, A. Frattini, L. Imberti, L. B. Gatta, H. D. Ochs, K. Schwarz, L. D. Notarangelo, P. Vezzoni, and E. Spanopoulou. 1998. Partial V(D)J recombination activity leads to Omenn syndrome. *Cell* 93:885.
 10. Villa, A., S. Santagata, F. Bozzi, L. Imberti, and L. D. Notarangelo. 1999. Omenn syndrome: a disorder of Rag1 and Rag2 genes. *J. Clin. Immunol.* 19:87.
 11. Spanopoulou, E., F. Zaitseva, F. H. Wang, S. Santagata, D. Baltimore, and G. Panayotou. 1996. The homeodomain region of Rag-1 reveals the parallel mechanisms of bacterial and V(D)J recombination. *Cell* 87:263.
 12. Difilippantonio, M. J., C. J. McMahan, Q. M. Eastman, E. Spanopoulou, and D. G. Schatz. 1996. RAG1 mediates signal sequence recognition and recruitment of RAG2 in V(D)J recombination. *Cell* 87:253.
 13. Swanson, P. C., and S. Desiderio. 1998. V(D)J recombination signal recognition: distinct, overlapping DNA-protein contacts in complexes containing RAG1 with and without RAG2. *Immunity* 9:115.
 14. Nagawa, F., K. Ishiguro, A. Tsuboi, T. Yoshida, A. Ishikawa, T. Takemori, A. J. Otsuka, and H. Sakano. 1998. Footprint analysis of the RAG protein recombination signal sequence complex for V(D)J type recombination. *Mol. Cell. Biol.* 18:655.
 15. Akamatsu, Y., and M. A. Oettinger. 1998. Distinct roles of RAG1 and RAG2 in binding the V(D)J recombination signal sequences. *Mol. Cell. Biol.* 18:4670.
 16. Landree, M. A., J. A. Wibbenmeyer, and D. B. Roth. 1999. Mutational analysis of RAG1 and RAG2 identifies three catalytic amino acids in RAG1 critical for both cleavage steps of V(D)J recombination. *Genes Dev.* 13:3059.
 17. Kim, D. R., Y. Dai, C. L. Mundy, Y. Yang, and M. A. Oettinger. 1999. Mutations of acidic residues in RAG1 define the active site of the V(D)J recombinase. *Genes Dev.* 13:3070.
 18. Fugmann, S. D., I. J. Villey, L. M. Ptaszek, and D. G. Schatz. 2000. Identification of two catalytic residues in RAG1 that define a single active site within the RAG1/RAG2 protein complex. *Mol. Cell* 5:97.
 19. Eastman, Q. M., I. J. Villey, and D. G. Schatz. 1999. Detection of RAG protein-V(D)J recombination signal interactions near the site of DNA cleavage by UV cross-linking. *Mol. Cell. Biol.* 19:3788.
 20. Swanson, P. C., and S. Desiderio. 1999. RAG-2 promotes heptamer occupancy by RAG-1 in the assembly of a V(D)J initiation complex. *Mol. Cell. Biol.* 19:3674.
 21. Hiom, K., and M. Gellert. 1997. A stable RAG1-RAG2-DNA complex that is active in V(D)J cleavage. *Cell* 88:65.
 22. Santagata, S., V. Aidinis, and E. Spanopoulou. 1998. The effect of Me^{2+} cofactors at the initial stages of V(D)J recombination. *J. Biol. Chem.* 273:16325.
 23. Aidinis, V., T. Bonaldi, M. Beltrame, S. Santagata, M. E. Bianchi, and E. Spanopoulou. 1999. The RAG1 homeodomain recruits HMG1 and HMG2 to facilitate recombination signal sequence binding and to enhance the intrinsic DNA-bending activity of RAG1-RAG2. *Mol. Cell. Biol.* 19:6532.
 24. McBlane, J. F., D. C. van Gent, D. A. Ramsden, C. Romeo, C. A. Cuomo, M. Gellert, and M. A. Oettinger. 1995. Cleavage at a V(D)J recombination signal requires only RAG1 and RAG2 proteins and occurs in two steps. *Cell* 83:387.
 25. Besmer, E., J. Mansilla-Soto, S. Cassard, D. J. Sawchuk, G. Brown, M. Sadofsky, S. M. Lewis, M. C. Nussenzweig, and P. Cortes. 1998. Hairpin coding end opening is mediated by RAG1 and RAG2 proteins. *Mol. Cell* 2:817.
 26. Shockett, P. E., and D. G. Schatz. 1999. DNA hairpin opening mediated by the RAG1 and RAG2 proteins. *Mol. Cell. Biol.* 19:4159.
 27. Santagata, S., E. Besmer, A. Villa, F. Bozzi, J. S. Allingham, C. Sobacchi, D. B. Haniford, P. Vezzoni, M. C. Nussenzweig, Z. Q. Pan, and P. Cortes. 1999. The RAG1/RAG2 complex constitutes a 3' flap endonuclease: implications for junctional diversity in V(D)J and transpositional recombination. *Mol. Cell* 4:935.
 28. Sadofsky, M. J., J. E. Hesse, J. F. McBlane, and M. Gellert. 1993. Expression and V(D)J recombination activity of mutated RAG-1 proteins. [Published erratum appears in 1994 *Nucleic Acids Res.* 22:550.] *Nucleic Acids Res.* 21:5644.
 29. Cuomo, C. A., and M. A. Oettinger. 1994. Analysis of regions of RAG-2 important for V(D)J recombination. *Nucleic Acids Res.* 22:1810.
 30. Eastman, Q. M., T. M. Leu, and D. G. Schatz. 1996. Initiation of V(D)J recombination in vitro obeying the 12/23 rule. *Nature* 380:85.
 31. van Gent, D. C., D. A. Ramsden, and M. Gellert. 1996. The RAG1 and RAG2 proteins establish the 12/23 rule in V(D)J recombination. *Cell* 85:107.
 32. Eastman, Q. M., and D. G. Schatz. 1997. Nicking is asynchronous and stimulated by synapsis in 12/23 rule-regulated V(D)J cleavage. *Nucleic Acids Res.* 25:4370.
 33. Hiom, K., and M. Gellert. 1998. Assembly of a 12/23 paired signal complex: a critical control point in V(D)J recombination. *Mol. Cell* 1:1011.
 34. Kim, D. R., and M. A. Oettinger. 1998. Functional analysis of coordinated cleavage in V(D)J recombination. *Mol. Cell. Biol.* 18:4679.
 35. West, R. B., and M. R. Lieber. 1998. The RAG-HMG1 complex enforces the 12/23 rule of V(D)J recombination specifically at the double-hairpin formation step. *Mol. Cell. Biol.* 18:6408.
 36. Agrawal, A., and D. G. Schatz. 1997. RAG1 and RAG2 form a stable postcleavage synaptic complex with DNA containing signal ends in V(D)J recombination. *Cell* 89:43.
 37. Agrawal, A., Q. M. Eastman, and D. G. Schatz. 1998. Transposition mediated by RAG1 and RAG2 and its implications for the evolution of the immune system. *Nature* 394:744.
 38. Hiom, K., M. Melek, and M. Gellert. 1998. DNA transposition by the RAG1 and RAG2 proteins: a possible source of oncogenic translocations. *Cell* 94:463.
 39. Spanopoulou, E., P. Cortes, C. Shih, C. M. Huang, D. P. Silver, P. Svec, and D. Baltimore. 1995. Localization, interaction, and RNA binding properties of the V(D)J recombination-activating proteins RAG1 and RAG2. *Immunity* 3:715.
 40. McMahan, C. J., M. J. Sadofsky, and D. G. Schatz. 1997. Definition of a large region of RAG1 that is important for coimmunoprecipitation of RAG2. *J. Immunol.* 158:2202.
 41. Mo, X., T. Bailin, and M. J. Sadofsky. 1999. RAG1 and RAG2 cooperate in specific binding to the recombination signal sequence in vitro. *J. Biol. Chem.* 274:7025.
 42. Callebaut, I., and J. P. Mornon. 1998. The V(D)J recombination activating protein RAG2 consists of a six-bladed propeller and a PHD fingerlike domain, as revealed by sequence analysis. *Cell. Mol. Life Sci.* 54:880.
 43. Aravind, L., and E. V. Koonin. 1999. Gleaning non-trivial structural, functional and evolutionary information about proteins by iterative database searches. *J. Mol. Biol.* 287:1023.
 44. Lieber, M. R., J. E. Hesse, S. Lewis, G. C. Bosma, N. Rosenberg, K. Mizuuchi, M. J. Bosma, and M. Gellert. 1988. The defect in murine severe combined immune deficiency: joining of signal sequences but not coding segments in V(D)J recombination. *Cell* 55:7.
 45. Cortes, P., F. Weis-Garcia, Z. Misulovin, A. Nussenzweig, J. S. Lai, G. Li, M. C. Nussenzweig, and D. Baltimore. 1996. In vitro V(D)J recombination: signal joint formation. *Proc. Natl. Acad. Sci. USA* 93:14008.
 46. Weis-Garcia, F., E. Besmer, D. J. Sawchuk, W. Yu, Y. Hu, S. Cassard, M. C. Nussenzweig, and P. Cortes. 1997. V(D)J recombination: in vitro coding joint formation. *Mol. Cell. Biol.* 17:6379.
 47. Lai, J. S., and W. Herr. 1992. Ethidium bromide provides a simple tool for identifying genuine DNA-independent protein associations. *Proc. Natl. Acad. Sci. USA* 89:6958.
 48. Ito, N., S. E. Phillips, C. Stevens, Z. B. Ogel, M. J. McPherson, J. N. Keen, K. D. Yadav, and P. F. Knowles. 1991. Novel thioether bond revealed by a 1.7 Å crystal structure of galactose oxidase. *Nature* 350:87.
 49. Bork, P., and R. F. Doolittle. 1994. *Drosophila* kelch motif is derived from a common enzyme fold. *J. Mol. Biol.* 236:1277.
 50. Way, M., M. Sanders, M. Chafel, Y. H. Tu, A. Knight, and P. Matsudaira. 1995. β -Scruiin, a homologue of the actin crosslinking protein scruiin, is localized to the acrosomal vesicle of *Limulus* sperm. *J. Cell Sci.* 108:3155.
 51. Philips, J., and I. Herskowitz. 1998. Identification of Kellp, a kelch domain-containing protein involved in cell fusion and morphology in *Saccharomyces cerevisiae*. *J. Cell Biol.* 143:375.
 52. Xue, F., and L. Cooley. 1993. Kelch encodes a component of intercellular bridges in *Drosophila* egg chambers. *Cell* 72:681.
 53. Chang-Yeh, A., D. E. Mold, and R. C. Huang. 1991. Identification of a novel murine IAP-promoted placenta-expressed gene. *Nucleic Acids Res.* 19:3667.
 54. Robinson, D. N., and L. Cooley. 1997. *Drosophila* kelch is an oligomeric ring canal actin organizer. *J. Cell Biol.* 138:799.
 55. Sanders, M. C., M. Way, J. Sakai, and P. Matsudaira. 1996. Characterization of the actin cross-linking properties of the scruiin-calmodulin complex from the acrosomal process of *Limulus* sperm. *J. Biol. Chem.* 271:2651.
 56. Sadofsky, M. J., J. E. Hesse, and M. Gellert. 1994. Definition of a core region of RAG-2 that is functional in V(D)J recombination. *Nucleic Acids Res.* 22:1805.
 57. Rice, P., and K. Mizuuchi. 1995. Structure of the bacteriophage Mu transposase core: a common structural motif for DNA transposition and retroviral integration. *Cell* 82:209.
 58. Tamura, K., W. S. Shan, W. A. Hendrickson, D. R. Colman, and L. Shapiro. 1998. Structure-function analysis of cell adhesion by neural (N-) cadherin. *Neuron* 20:1153.
 59. Rodgers, K. K., Z. Bu, K. G. Fleming, D. G. Schatz, D. M. Engelman, and J. E. Coleman. 1996. A zinc-binding domain involved in the dimerization of RAG1. *J. Mol. Biol.* 260:70.
 60. Bellon, S. F., K. K. Rodgers, D. G. Schatz, J. E. Coleman, and T. A. Steitz. 1997. Crystal structure of the RAG1 dimerization domain reveals multiple zinc-binding motifs including a novel zinc binuclear cluster. *Nat. Struct. Biol.* 4:586.